

Original article

DOI: <https://doi.org/10.18721/JPM.15210>

## CALCULATION OF MIXED MODE STRESS INTENSITY FACTORS FOR ORTHOTROPIC MATERIALS IN THE PLANE STRESS STATE

*A. V. Savikovskii* , *A. S. Semenov*

Peter the Great St. Petersburg Polytechnic University, St. Petersburg, Russia

 [savikovskij.av@edu.spbstu.ru](mailto:savikovskij.av@edu.spbstu.ru)

**Abstract.** In the article, stress intensity factors for a straight crack of a mixed-fracture mode in the orthotropic material and in its particular case, namely, in the material with cubic symmetry, have been calculated. The displacement and stress extrapolation method based on the Lekhnitskii formalism was used. For considered classes of materials, the explicit expressions for influence matrix elements were obtained through the elastic constants of the material in the cases of its planar-stressed state and given a non-zero angle between the material's anisotropy and the crack's axes. Influence matrix properties were analyzed systematically. The obtained results of verification of considered variants of the displacement and stress extrapolation method exhibited a good agreement between the numerical and analytical solutions (the difference did not exceed 0.8 %).

**Keywords:** Lekhnitskii formalism, orthotropic material, stress intensity factor, mixed-mode fracture

**Citation:** Savikovskii A. V., Semenov A. S., Calculation of mixed-mode stress intensity factors for orthotropic materials in the plane stress state, St. Petersburg Polytechnical State University Journal. Physics and Mathematics. 15 (2) (2022) 102–123. DOI: <https://doi.org/10.18721/JPM.15210>

This is an open access article under the CC BY-NC 4.0 license (<https://creativecommons.org/licenses/by-nc/4.0/>)



Научная статья

УДК 539.3, 539.42

DOI: <https://doi.org/10.18721/JPM.15210>

## ВЫЧИСЛЕНИЕ КОЭФФИЦИЕНТОВ ИНТЕНСИВНОСТИ НАПРЯЖЕНИЙ В ОРТОТРОПНЫХ МАТЕРИАЛАХ ПРИ СМЕШАННОЙ МОДЕ РАЗРУШЕНИЯ В ПЛОСКОМ НАПРЯЖЕННОМ СОСТОЯНИИ

*А. В. Савиковский* , *А. С. Семенов*

Санкт-Петербургский политехнический университет Петра Великого, Санкт-Петербург, Россия

 [savikovskij.av@edu.spbstu.ru](mailto:savikovskij.av@edu.spbstu.ru)

**Аннотация.** Статья посвящена вычислению коэффициентов интенсивности напряжений для прямолинейной трещины смешанной моды разрушения в ортотропном материале и его частном случае – материале с кубической симметрией. Использован метод экстраполяции перемещений и напряжений на основе формализма Лехницкого. Для рассмотренных классов материалов получены в явном виде выражения для элементов матрицы влияния через упругие константы материала в случаях его плосконапряженного состояния и наличия ненулевого угла между осями анизотропии материала и трещины. Систематически проанализированы свойства матрицы влияния. Полученные результаты верификации рассмотренных вариантов метода перемещений и напряжений показали хорошее согласие между численными и аналитическими решениями (отличие не превосходит 0.8%).

**Ключевые слова:** формализм Лехницкого, ортотропный материал, коэффициент интенсивности напряжений, смешанная мода разрушения

**Для цитирования:** Савиковский А. В., Семенов А. С. Вычисление коэффициентов интенсивности напряжений в ортотропных материалах при смешанной моде разрушения в плоском напряженном состоянии // Научно-технические ведомости СПбГПУ. Физико-математические науки. 2022. Т. 2 № .15. С. 102–123. DOI: <https://doi.org/10.18721/JPM.15210>

Статья открытого доступа, распространяемая по лицензии CC BY-NC 4.0 (<https://creativecommons.org/licenses/by-nc/4.0/>)

### Introduction

Heat-resistant single-crystal nickel-based alloys [1–3] are widely used as a structural material for critical components (primarily blades) of gas turbine engines (GTE) [4–7] operating at temperatures above 1000 °C [8, 9]. Microstructurally, heat-resistant nickel alloys consist of an  $\gamma$ -phase (a Ni-based solid solution) and a strengthening  $\gamma'$ -phase [1, 4, 7]. Single-crystal nickel alloys have cubic symmetry of thermoelastic properties and can be regarded as a particular case of an orthotropic material with isotropic properties along the crystallographic axes [100], [010] and [001].

Cooled GTE blades made of heat-resistant nickel alloys are the most loaded elements in the engine [10–15], acted on by centrifugal forces and gas pressure, as well as unsteady and non-uniform temperature fields. Different kinds of combined variable loads induce fatigue, creep and thermal cracks in GTE blades [4, 16, 17].

The phenomena of thermal fatigue, initiation and propagation of cracks in single-crystal Ni alloys are often studied experimentally, for example, in hourglass specimens [4]. The initiation of a thermal fatigue crack in an hourglass specimen was simulated in [18, 19] by the finite element method (FEM). Evaluating crack resistance in nickel alloys and constructing approaches to calculating fracture parameters in the cases of cubic symmetry and orthotropic materials is a crucial challenge that is yet to be addressed conclusively.

We consider the stress intensity factors (SIFs) as the main fracture parameters in this study. In general, SIF calculations in anisotropic materials should be supported by analysis of mixed fracture modes.

The goal of this study consisted in obtaining explicit formulas for calculating the SIF in terms of crack edge displacements in the vicinity of the crack tip.

A numerical method is used for this purpose, extrapolating the displacements to the crack tip in a material with cubic symmetry and in an orthotropic material. A stress extrapolation method is also considered as an example.

The Lekhnitskii formalism is an effective technique used to achieve this [20]. We verified the proposed relations, testing the stress extrapolation method for isotropic and orthotropic materials, as well as for a material with cubic symmetry.

### Constitutive equations

The constitutive equations for a linear elastic material take the following form [21, 22]:

$$\boldsymbol{\varepsilon} = {}^4\mathbf{S} \cdot \boldsymbol{\sigma}, \quad (1)$$

where  $\boldsymbol{\varepsilon}$  is the strain tensor,  $\boldsymbol{\sigma}$  is the stress tensor,  ${}^4\mathbf{S}$  is the elastic compliance tensor of the material.

System of linear equations (1) can be conveniently rewritten in matrix form:

$$\{\boldsymbol{\varepsilon}\} = [\mathbf{S}]\{\boldsymbol{\sigma}\}, \quad (2)$$

where the notations for vector columns composed of tensor components are introduced:

$$\{\boldsymbol{\varepsilon}\} = \begin{Bmatrix} \varepsilon_{xx} \\ \varepsilon_{yy} \\ \varepsilon_{zz} \\ \gamma_{yz} \\ \gamma_{xz} \\ \gamma_{xy} \end{Bmatrix} \quad \text{and} \quad \{\boldsymbol{\sigma}\} = \begin{Bmatrix} \sigma_{xx} \\ \sigma_{yy} \\ \sigma_{zz} \\ \sigma_{yz} \\ \sigma_{xz} \\ \sigma_{xy} \end{Bmatrix}.$$

The order in which the components are listed corresponds to the Voigt notation.

The 6×6 elastic compliance matrix  $[\mathbf{S}]$  corresponding to the compliance tensor  ${}^4\mathbf{S}$  has a different form for materials with different structures.

Case of orthotropic material:

$$[\mathbf{S}] = \begin{pmatrix} \frac{1}{E_1} & -\frac{\nu_{12}}{E_1} & -\frac{\nu_{13}}{E_1} & 0 & 0 & 0 \\ -\frac{\nu_{12}}{E_1} & \frac{1}{E_2} & -\frac{\nu_{23}}{E_2} & 0 & 0 & 0 \\ -\frac{\nu_{13}}{E_1} & -\frac{\nu_{23}}{E_2} & \frac{1}{E_3} & 0 & 0 & 0 \\ 0 & 0 & 0 & \frac{1}{G_{23}} & 0 & 0 \\ 0 & 0 & 0 & 0 & \frac{1}{G_{13}} & 0 \\ 0 & 0 & 0 & 0 & 0 & \frac{1}{G_{12}} \end{pmatrix}, \quad (3)$$

where  $E_1, E_2, E_3$  are Young's moduli;  $G_{23}, G_{13}, G_{12}$  are shear moduli;  $\nu_{23}, \nu_{13}, \nu_{12}$  are Poisson's ratios.

Case of cubic symmetry:

$$[\mathbf{S}] = \begin{pmatrix} \frac{1}{E} & -\frac{\nu}{E} & -\frac{\nu}{E} & 0 & 0 & 0 \\ -\frac{\nu}{E} & \frac{1}{E} & -\frac{\nu}{E} & 0 & 0 & 0 \\ -\frac{\nu}{E} & -\frac{\nu}{E} & \frac{1}{E} & 0 & 0 & 0 \\ 0 & 0 & 0 & \frac{1}{G} & 0 & 0 \\ 0 & 0 & 0 & 0 & \frac{1}{G} & 0 \\ 0 & 0 & 0 & 0 & 0 & \frac{1}{G} \end{pmatrix}. \quad (4)$$

Case of isotropic material:

$$[\mathbf{S}] = \begin{pmatrix} \frac{1}{E} & -\frac{\nu}{E} & -\frac{\nu}{E} & 0 & 0 & 0 \\ -\frac{\nu}{E} & \frac{1}{E} & -\frac{\nu}{E} & 0 & 0 & 0 \\ -\frac{\nu}{E} & -\frac{\nu}{E} & \frac{1}{E} & 0 & 0 & 0 \\ 0 & 0 & 0 & \frac{2(1+\nu)}{E} & 0 & 0 \\ 0 & 0 & 0 & 0 & \frac{2(1+\nu)}{E} & 0 \\ 0 & 0 & 0 & 0 & 0 & \frac{2(1+\nu)}{E} \end{pmatrix}. \quad (5)$$

where  $E$  is Young's modulus,  $G$  is the shear modulus,  $\nu$  is Poisson's ratio.

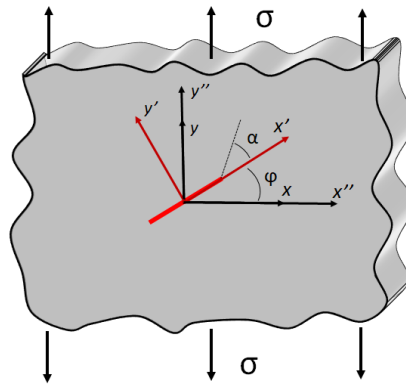


Fig. 1. Schematic diagram of uniaxial tension in the orthotropic plane with a single oblique straight crack (marked with a red line):

$x, y$  are the axes of the global coordinate system;  $x', y'$  are the axes of the crack coordinate system;  $x'', y''$  are the anisotropy axes of the material;  $\varphi$  is the crack orientation angle,  $\alpha$  is the angle between the direction to the point and the crack axis; the arrows indicate the loading direction ( $\sigma$  is the uniaxial tensile stress)

### Numerical methods for finding the SIF and the Lekhnitskii formalism

We consider the problem on uniaxial tension in an orthotropic plane (plate) with a single oblique straight crack assuming a plane stress state. The axes of the coordinate system introduced coincide with the anisotropy axes of the material and the loading direction. The orientation of the crack does not coincide with the anisotropy axes of the material and the loading direction (Fig. 1).

Asymptotic expressions for displacements in the vicinity of the crack tip in the general three-dimensional case for three fracture modes (non-zero values of the coefficients  $K_I, K_{II}, K_{III}$ ) are represented for isotropic material by the relations given in monograph [22]. Similar expressions for anisotropic material are obtained using the Lekhnitskii formalism; they have the following form [23–25]:

$$\begin{aligned}
 u_x(r, \alpha) &= \frac{K_I \sqrt{2r}}{\sqrt{\pi}} \cdot \operatorname{Re} \left( \frac{1}{\mu'_1 - \mu'_2} \left( \mu'_1 p_2 \sqrt{\cos \alpha + \mu'_2 \sin \alpha} - \mu'_2 p_1 \sqrt{\cos \alpha + \mu'_1 \sin \alpha} \right) \right) + \\
 &+ \frac{K_{II} \sqrt{2r}}{\sqrt{\pi}} \cdot \operatorname{Re} \left( \frac{1}{\mu'_1 - \mu'_2} \left( p_2 \sqrt{\cos \alpha + \mu'_2 \sin \alpha} - p_1 \sqrt{\cos \alpha + \mu'_1 \sin \alpha} \right) \right), \\
 u_y(r, \alpha) &= \frac{K_I \sqrt{2r}}{\sqrt{\pi}} \cdot \operatorname{Re} \left( \frac{1}{\mu'_1 - \mu'_2} \left( \mu'_1 q_2 \sqrt{\cos \alpha + \mu'_2 \sin \alpha} - \mu'_2 q_1 \sqrt{\cos \alpha + \mu'_1 \sin \alpha} \right) \right) + \\
 &+ \frac{K_{II} \sqrt{2r}}{\sqrt{\pi}} \cdot \operatorname{Re} \left( \frac{1}{\mu'_1 - \mu'_2} \left( q_2 \sqrt{\cos \alpha + \mu'_2 \sin \alpha} - q_1 \sqrt{\cos \alpha + \mu'_1 \sin \alpha} \right) \right), \\
 u_z(r, \alpha) &= \frac{K_{III} \sqrt{2r}}{\sqrt{\pi}} \cdot \operatorname{Re} \left( \frac{\sqrt{\cos \alpha + \mu'_3 \sin \alpha}}{C'_{45} + \mu_3 C'_{44}} \right),
 \end{aligned} \tag{6}$$

where  $u_x(r, \alpha), u_y(r, \alpha), u_z(r, \alpha)$  are the axial displacements in the coordinate system of the crack;  $K_I, K_{II}, K_{III}$  are the SIFs for fracture modes I, II, III;  $G$  is the shear modulus;  $r$  is the distance from the crack tip to the given point;  $\alpha$  is the angle between the direction to the point and the crack axis;  $\nu$  is Poisson's ratio;  $C'_{ij}$  are the constants of the material's stiffness matrix in the coordinate system of the crack,  $[C] = [S]^{-1}$ ;  $p_i = S'_{11} \mu_i^2 + S'_{12} - S'_{16} \mu_i$ ,  $q_i = S'_{12} \mu_i + S'_{22} / \mu_i - S'_{26} \mu_i$  ( $S'_{ij}$  are the constants of the material's compliance matrix in the coordinate system of the crack);  $\mu'_1, \mu'_2$  are the roots of the 4<sup>th</sup>-order equation taking the form



$$S'_{11}\mu^4 - 2S'_{16}\mu^3 + (2S'_{12} + S'_{66})\mu^2 - 2S'_{26}\mu + S'_{22} = 0, \quad (7)$$

with a positive imaginary part;  $\mu'_3$  is the root of the equation

$$C'_{44}\mu^2 - 2C'_{45}\mu + C'_{55} = 0,$$

also with a positive imaginary part.

Displacements along the free edges of the crack are determined using the expressions presented in monograph [22], where the angle between the direction to the point and the crack axis  $\alpha$  is taken equal to  $\pi$ . The obtained expressions can be used to find the SIF values in terms of crack edge displacements; if the material is isotropic, they take the form

$$\begin{aligned} K_I &= u_y(r, \pi) \sqrt{\frac{2\pi}{r}} \cdot \frac{2G}{1+\kappa}, \\ K_{II} &= u_x(r, \pi) \sqrt{\frac{2\pi}{r}} \cdot \frac{2G}{1+\kappa}, \\ K_{III} &= u_z(r, \pi) \sqrt{\frac{2\pi}{r}} \cdot G. \end{aligned} \quad (8)$$

If the material is anisotropic, substituting  $\alpha = \pi$  in expression (6), we obtain an equation of the form

$$\{\mathbf{u}\} = \sqrt{\frac{2r}{\pi}} [\mathbf{B}] \cdot \{\mathbf{K}\}, \quad (9)$$

where  $\{\mathbf{u}\} = \begin{Bmatrix} u_x(r, \pi) \\ u_y(r, \pi) \\ u_z(r, \pi) \end{Bmatrix}$ ,  $\{\mathbf{K}\} = \begin{Bmatrix} K_I \\ K_{II} \\ K_{III} \end{Bmatrix}$ ;

$$[\mathbf{B}] = \begin{pmatrix} \operatorname{Re}\left(\frac{\mu'_1 p_2 - \mu'_2 p_1}{\mu'_1 - \mu'_2} i\right) & \operatorname{Re}\left(\frac{p_2 - p_1}{\mu'_1 - \mu'_2} i\right) & 0 \\ \operatorname{Re}\left(\frac{\mu'_1 q_2 - \mu'_2 q_1}{\mu'_1 - \mu'_2} i\right) & \operatorname{Re}\left(\frac{q_2 - q_1}{\mu'_1 - \mu'_2} i\right) & 0 \\ 0 & 0 & \frac{1}{\sqrt{C'_{44} C'_{55} - C'^2_{45}}} \end{pmatrix} \text{ is a } 3 \times 3 \text{ influence matrix for}$$

three components in the vector of the crack's relative edge displacement versus three SIFs.

Inverting Eq. (9) allows to calculate the SIF in terms of the edge displacements for the case of anisotropic material [26, 27]:

$$\{\mathbf{K}\} = \sqrt{\frac{\pi}{2r}} \cdot [\mathbf{B}]^{-1} \cdot \{\mathbf{u}\}, \quad (10)$$

$$\text{where } [\mathbf{B}]^{-1} = \begin{pmatrix} \frac{1}{\det[\mathbf{D}]} \operatorname{Re}\left(\frac{\mu'_1 p_2 - \mu'_2 p_1}{\mu'_1 - \mu'_2} i\right) & \frac{1}{\det[\mathbf{D}]} \operatorname{Re}\left(-\frac{p_2 - p_1}{\mu'_1 - \mu'_2} i\right) & 0 \\ \frac{1}{\det[\mathbf{D}]} \operatorname{Re}\left(-\frac{\mu'_1 q_2 - \mu'_2 q_1}{\mu'_1 - \mu'_2} i\right) & \frac{1}{\det[\mathbf{D}]} \operatorname{Re}\left(\frac{q_2 - q_1}{\mu'_1 - \mu'_2} i\right) & 0 \\ 0 & 0 & \sqrt{C'_{44} C'_{55} - C'^2_{45}} \end{pmatrix}, \quad (11)$$

$$\det[\mathbf{D}] = \begin{vmatrix} \operatorname{Re}\left(\frac{\mu'_1 p_2 - \mu'_2 p_1}{\mu'_1 - \mu'_2} i\right) & \operatorname{Re}\left(\frac{p_2 - p_1}{\mu'_1 - \mu'_2} i\right) \\ \operatorname{Re}\left(\frac{\mu'_1 q_2 - \mu'_2 q_1}{\mu'_1 - \mu'_2} i\right) & \operatorname{Re}\left(\frac{q_2 - q_1}{\mu'_1 - \mu'_2} i\right) \end{vmatrix}.$$

Notably, if the coordinate system of the crack does not coincide with the anisotropy axes of the material (which is what happens in mixed fracture mode), the constants of the compliance and stiffness matrices must be converted to the coordinate system of the crack, while the roots  $\mu'_1, \mu'_2$  must be found from the 4<sup>th</sup>-order equation with compliance constants in the coordinate system of the crack.

If the coordinate system is rotated, the transition matrix from one coordinate system to the other for rotation in the plane by the angle  $\varphi$  has the form

$$Q = \begin{pmatrix} \cos \varphi & \sin \varphi & 0 \\ -\sin \varphi & \cos \varphi & 0 \\ 0 & 0 & 1 \end{pmatrix}$$

and the equation for transforming the elements of the elastic compliance tensor and 4<sup>th</sup>-order elastic moduli from the initial to the new coordinate system has the following form:

$$\begin{aligned} S'_{ijkl} &= Q_{im} \cdot Q_{jn} \cdot Q_{ko} \cdot Q_{lp} \cdot S_{mnop}, \\ C'_{ijkl} &= Q_{im} \cdot Q_{jn} \cdot Q_{ko} \cdot Q_{lp} \cdot C_{mnop}, \end{aligned} \tag{12}$$

where  $S_{mnop}, S'_{ijkl}$  are the elements of the compliance tensor in the initial and rotated (associated with the crack) coordinate systems, respectively;  $C_{mnop}, C'_{ijkl}$  are the elements of the stiffness tensor in the initial and rotated (associated with the crack) coordinate systems, respectively.

To use Eqs. (8) and (10), the displacements must also be converted from the global coordinate system to the coordinate system associated with the crack.

Rotating the plane at an angle  $\varphi$  for the case of an orthotropic material and transforming the tensors of elastic moduli, elastic compliances and rotation into  $6 \times 6$  matrices (since  $S_{16} = S_{26} = S_{45} = 0$  for the orthotropic material), then Eqs. (12) take the form given by Lekhnitskii [20, 28].

Thus, provided that the displacements of the crack edges and the elastic properties of the material are known, the SIF can be calculated by the displacement method.

Asymptotic expressions for stresses near the crack tip in the three-dimensional case, when the fracture modes I, II and III are observed, and the factors  $K_I, K_{II}, K_{III}$  are determined for the isotropic material by the relations [22, 29]. Considering the stresses on the path along which the crack grows in the vicinity of the crack tip, i.e., at  $\alpha = 0$ , and expressing the SIFs in terms of stresses, we obtain the following expressions for the isotropic material:

$$\begin{aligned} K_I &= \sigma_{yy}(r, 0) \cdot \sqrt{2\pi r}, \\ K_{II} &= \sigma_{xy}(r, 0) \cdot \sqrt{2\pi r}, \\ K_{III} &= \sigma_{yz}(r, 0) \cdot \sqrt{2\pi r}. \end{aligned} \tag{13}$$

Asymptotic expressions derived based on the Lekhnitskii formalism for stresses near the crack tip in the three-dimensional case take the following form for the anisotropic material [23–25, 30, 31]:



$$\begin{aligned}
 \sigma_{xx}(r, \alpha) &= \frac{K_I}{\sqrt{2\pi r}} \cdot \operatorname{Re} \left( \frac{\mu'_1 \mu'_2}{\mu'_1 - \mu'_2} \left( \frac{\mu'_2}{\sqrt{\cos \alpha + \mu'_2 \sin \alpha}} - \frac{\mu'_1}{\sqrt{\cos \alpha + \mu'_1 \sin \alpha}} \right) \right) + \\
 &+ \frac{K_{II}}{\sqrt{2\pi r}} \cdot \operatorname{Re} \left( \frac{1}{\mu'_1 - \mu'_2} \left( \frac{\mu_2'^2}{\sqrt{\cos \alpha + \mu'_2 \sin \alpha}} - \frac{\mu_1'^2}{\sqrt{\cos \alpha + \mu'_1 \sin \alpha}} \right) \right), \\
 \sigma_{yy}(r, \alpha) &= \frac{K_I}{\sqrt{2\pi r}} \cdot \operatorname{Re} \left( \frac{1}{\mu'_1 - \mu'_2} \left( \frac{\mu'_1}{\sqrt{\cos \alpha + \mu'_2 \sin \alpha}} - \frac{\mu'_2}{\sqrt{\cos \alpha + \mu'_1 \sin \alpha}} \right) \right) + \\
 &+ \frac{K_{II}}{\sqrt{2\pi r}} \cdot \operatorname{Re} \left( \frac{1}{\mu'_1 - \mu'_2} \left( \frac{1}{\sqrt{\cos \alpha + \mu'_2 \sin \alpha}} - \frac{1}{\sqrt{\cos \alpha + \mu'_1 \sin \alpha}} \right) \right), \\
 \sigma_{xy}(r, \alpha) &= \frac{K_I}{\sqrt{2\pi r}} \cdot \operatorname{Re} \left( \frac{\mu'_1 \mu'_2}{\mu'_1 - \mu'_2} \left( \frac{1}{\sqrt{\cos \alpha + \mu'_2 \sin \alpha}} - \frac{1}{\sqrt{\cos \alpha + \mu'_1 \sin \alpha}} \right) \right) + \\
 &+ \frac{K_{II}}{\sqrt{2\pi r}} \cdot \operatorname{Re} \left( \frac{1}{\mu'_1 - \mu'_2} \left( \frac{\mu'_1}{\sqrt{\cos \alpha + \mu'_2 \sin \alpha}} - \frac{\mu'_2}{\sqrt{\cos \alpha + \mu'_1 \sin \alpha}} \right) \right), \\
 \sigma_{xz}(r, \alpha) &= -\frac{K_{III}}{\sqrt{2\pi r}} \cdot \operatorname{Re} \left( \frac{\mu'_3}{\sqrt{\cos \alpha + \mu'_3 \sin \alpha}} \right), \quad \sigma_{yz}(r, \alpha) = \frac{K_{III}}{\sqrt{2\pi r}} \cdot \operatorname{Re} \left( \frac{\mu'_3}{\sqrt{\cos \alpha + \mu'_3 \sin \alpha}} \right),
 \end{aligned} \tag{14}$$

where  $\sigma_{ij}(r, \alpha)$  are the components of the stress tensor in the coordinate system of the crack.

Considering expressions (14) at  $\alpha = 0$  and expressing the SIFs in terms of stresses, we obtain the equations coinciding with the isotropic case for the anisotropic material:

$$\begin{aligned}
 K_I &= \sigma_{yy}(r, 0) \cdot \sqrt{2\pi r}, \\
 K_{II} &= \sigma_{xy}(r, 0) \cdot \sqrt{2\pi r}, \\
 K_{III} &= \sigma_{yz}(r, 0) \cdot \sqrt{2\pi r}.
 \end{aligned} \tag{15}$$

Thus, we can use the stresses in the vicinity of the crack tip to find the SIFs for both isotropic and anisotropic materials, so that the resulting expressions are the same. Notably, if Eqs. (13)–(15) are used, the stresses must be converted to the coordinate system of the crack.

### Calculation of the matrix $[\mathbf{B}]^{-1}$ in terms of elastic moduli

We have established in the previous section that the SIF can be found from the displacements via Eq. (10) for the anisotropic material. Let us now obtain explicit expressions for the roots of the 4th-order equation and the matrix  $[\mathbf{B}]^{-1}$  in terms of the elastic moduli of the orthotropic material in the case of a plane stress state, when the crack is in the plane  $xy$ . Consider first the 4th-order equation (7), when the coordinate system of the crack coincides with the coordinate system of the material:

$$S_{11}\mu^4 - 2S_{16}\mu^3 + (2S_{12} + S_{66})\mu^2 - 2S_{26}\mu + S_{22} = 0, \tag{16}$$

We substitute the coefficients  $S_{ij}$  for the case of the plane stress state and multiply by  $E_1$ ; then, because Eq. (7) holds true, we obtain the equation:

$$\mu^4 + \left( \frac{E_1}{G_{12}} - 2\nu_{12} \right) \mu^2 + \frac{E_1}{E_2} = 0. \tag{17}$$



The roots of Eq. (17) depend on the elastic constants of the material. Thus, there are two cases for the roots of Eq. (17).

Case 1. If  $\left(\frac{E_1}{G_{12}} - 2\nu_{12}\right)^2 - 4\frac{E_1}{E_2} < 0$ , then the roots are expressed as follows:

$$\begin{aligned}\mu_1 &= A + iB, \\ \mu_2 &= -A + iB,\end{aligned}\tag{18}$$

$$\text{where } A = \frac{\sqrt{2\sqrt{\frac{E_1}{E_2}} - \left(\frac{E_1}{G_{12}} - 2\nu_{12}\right)}}{2}, \quad B = \frac{\sqrt{2\sqrt{\frac{E_1}{E_2}} + \left(\frac{E_1}{G_{12}} - 2\nu_{12}\right)}}{2}.$$

Case 2. If  $\left(\frac{E_1}{G_{12}} - 2\nu_{12}\right)^2 - 4\frac{E_1}{E_2} \geq 0$ , then the roots are expressed as follows:

$$\begin{aligned}\mu_1 &= i(b^* + a^*), \\ \mu_2 &= i(b^* - a^*),\end{aligned}\tag{19}$$

$$\text{where } b^* = \frac{\sqrt{\left(\frac{E_1}{G_{12}} - 2\nu_{12}\right) + 2\sqrt{\frac{E_1}{E_2}}}}{2}, \quad a^* = \frac{\sqrt{\left(\frac{E_1}{G_{12}} - 2\nu_{12}\right) - 2\sqrt{\frac{E_1}{E_2}}}}{2}.$$

To find the roots of the equation for the case when the coordinate system of the crack does not coincide with the coordinate system of the material, we should transform the roots obtained. If the coordinate system is rotated by the angle  $\varphi$ , the roots of the equation in the initial and rotated coordinate systems are related as follows [20]:

$$\begin{aligned}\mu'_1 &= \frac{\mu_1 \cos \varphi - \sin \varphi}{\cos \varphi + \mu_1 \sin \varphi}, \\ \mu'_2 &= \frac{\mu_2 \cos \varphi - \sin \varphi}{\cos \varphi + \mu_2 \sin \varphi}.\end{aligned}\tag{20}$$

Case 1. If  $\left(\frac{E_1}{G_{12}} - 2\nu_{12}\right)^2 - 4\frac{E_1}{E_2} < 0$ , then, substituting expression (18) into Eq. (20), we obtain after the transformations:

$$\begin{aligned}\mu'_1 &= \frac{A \cos 2\varphi + \frac{A^2 + B^2 - 1}{2} \sin 2\varphi}{\cos^2 \varphi + A \sin 2\varphi + (A^2 + B^2) \sin^2 \varphi} + i \frac{B}{\cos^2 \varphi + A \sin 2\varphi + (A^2 + B^2) \sin^2 \varphi}, \\ \mu'_2 &= \frac{-A \cos 2\varphi + \frac{A^2 + B^2 - 1}{2} \sin 2\varphi}{\cos^2 \varphi - A \sin 2\varphi + (A^2 + B^2) \sin^2 \varphi} + i \frac{B}{\cos^2 \varphi - A \sin 2\varphi + (A^2 + B^2) \sin^2 \varphi}.\end{aligned}\tag{21}$$

Case 2. If  $\left(\frac{E_1}{G_{12}} - 2\nu_{12}\right)^2 - 4\frac{E_1}{E_2} \geq 0$ , then, substituting expression (19) into Eq. (20), we obtain after the transformations:

$$\begin{aligned}\mu'_1 &= \frac{((b^* + a^*)^2 - 1) \sin \varphi \cos \varphi}{\cos^2 \varphi + (b^* + a^*)^2 \sin^2 \varphi} + i \frac{b^* + a^*}{\cos^2 \varphi + (b^* + a^*)^2 \sin^2 \varphi}, \\ \mu'_2 &= \frac{((b^* - a^*)^2 - 1) \sin \varphi \cos \varphi}{\cos^2 \varphi + (b^* - a^*)^2 \sin^2 \varphi} + i \frac{b^* - a^*}{\cos^2 \varphi + (b^* - a^*)^2 \sin^2 \varphi}.\end{aligned}\quad (22)$$

The matrix  $[\mathbf{B}]^{-1}$  is defined by expression (11). Simplifying the expressions by which the elements of the matrix  $[\mathbf{B}]^{-1}$  are calculated, we obtain:

$$\begin{aligned}\frac{p_2 - p_1}{(\mu'_1 - \mu'_2)} &= S'_{16} - S'_{11} \cdot (\mu'_1 + \mu'_2), \quad \frac{q_2 - q_1}{(\mu'_1 - \mu'_2)} = \frac{S'_{22}}{\mu'_1 \mu'_2} - S'_{12}, \\ \frac{\mu'_1 p_2 - \mu'_2 p_1}{(\mu'_1 - \mu'_2)} &= S'_{12} - S'_{11} \mu'_1 \mu'_2, \quad \frac{\mu'_1 q_2 - \mu'_2 q_1}{(\mu'_1 - \mu'_2)} = S'_{22} \frac{\mu'_1 + \mu'_2}{\mu'_1 \mu'_2} - S'_{26}.\end{aligned}\quad (23)$$

Substituting expressions (21) to (23) for the complex roots of the equation and given that

$$E_1 S'_{11} = 1 - A^2 \sin^2 2\varphi + \left(\sqrt{\frac{E_1}{E_2}} - 1\right)^2 \sin^4 \varphi + 2 \sin^2 \varphi \left(\sqrt{\frac{E_1}{E_2}} - 1\right),$$

we obtain the influence matrix  $[\mathbf{B}]^{-1}$  explicitly:

$$[\mathbf{B}]^{-1} = \begin{pmatrix} \frac{\sqrt{E_1 E_2}}{4B} \left(1 - \sqrt{\frac{E_1}{E_2}}\right) \sin 2\varphi & \frac{\sqrt{E_1 E_2}}{2B} \left(\sqrt{\frac{E_1}{E_2}} \sin^2 \varphi + \cos^2 \varphi\right) & 0 \\ \frac{\sqrt{E_1 E_2}}{2B} \left(\sqrt{\frac{E_1}{E_2}} \cos^2 \varphi + \sin^2 \varphi\right) & \frac{\sqrt{E_1 E_2}}{4B} \left(1 - \sqrt{\frac{E_1}{E_2}}\right) \sin 2\varphi & 0 \\ 0 & 0 & \sqrt{G_{13} G_{23}} \end{pmatrix}, \quad (24)$$

where  $B = \frac{\sqrt{2\sqrt{\frac{E_1}{E_2}} + \left(\frac{E_1}{G_{12}} - 2\nu_{12}\right)}}{2}$ ,  $\varphi$  is the rotation angle of the material's coordinate system into the crack's coordinate system.

Substituting equalities (22) to (23) for the complex roots of Eq. (16) and given that

$$E_1 S'_{11} = (\cos^2 \varphi + B_1^2 \sin^2 \varphi)(\cos^2 \varphi + A_1^2 \sin^2 \varphi),$$

we obtain the expressions for the matrix  $[\mathbf{B}]^{-1}$ , which coincide with Eqs. (24).

Thus, the form of the matrix  $[\mathbf{B}]^{-1}$  for Case 1 of roots (21) in Eq. (16) coincides with form (24) of the matrix  $[\mathbf{B}]^{-1}$  for Case 2 of roots (22) in Eq. (16).

The SIF for the plane stress state in the orthotropic material is calculated from the displacements based on the following relations:

$$\begin{aligned}
 K_I &= \sqrt{\frac{\pi}{2r}} \left( \frac{\sqrt{E_1 E_2}}{4B} \left( 1 - \sqrt{\frac{E_1}{E_2}} \right) \sin 2\varphi \cdot u_x + \frac{\sqrt{E_1 E_2}}{2B} \left( \sqrt{\frac{E_1}{E_2}} \sin^2 \varphi + \cos^2 \varphi \right) \cdot u_y \right), \\
 K_{II} &= \sqrt{\frac{\pi}{2r}} \left( \frac{\sqrt{E_1 E_2}}{2B} \left( \sqrt{\frac{E_1}{E_2}} \cos^2 \varphi + \sin^2 \varphi \right) \cdot u_x + \frac{\sqrt{E_1 E_2}}{4B} \left( 1 - \sqrt{\frac{E_1}{E_2}} \right) \sin 2\varphi \cdot u_y \right), \\
 K_{III} &= \sqrt{\frac{\pi}{2r}} \cdot \sqrt{G_{13} G_{23}} \cdot u_z,
 \end{aligned} \tag{25}$$

where  $B = \frac{\sqrt{2 \sqrt{\frac{E_1}{E_2}} + \left( \frac{E_1}{G_{12}} - 2\nu_{12} \right)}}{2}$ .

Thus, the matrix  $[\mathbf{B}]^{-1}$  is the same for any values that the elastic parameters take in the orthotropic material. We should note that each SIF ( $K_I$  and  $K_{II}$ ) in Eq. (25) depends on both displacement components  $u_x$  and  $u_y$ .

An important practical case concerns calculating the SIF for single-crystal blades of gas turbines, which have a cubic elasticity. In this case, Eqs. (25) are simplified as follows ( $E_1 = E_2 = E$ ,  $G_{12} = G_{13} = G_{23} = G$ ):

$$\begin{aligned}
 K_I &= \sqrt{\frac{\pi}{2r}} \cdot \frac{E}{\sqrt{2 + \left( \frac{E}{G} - 2\nu \right)}} \cdot u_y, \\
 K_{II} &= \sqrt{\frac{\pi}{2r}} \cdot \frac{E}{\sqrt{2 + \left( \frac{E}{G} - 2\nu \right)}} \cdot u_x, \\
 K_{III} &= \sqrt{\frac{\pi}{2r}} \cdot G \cdot u_z.
 \end{aligned} \tag{26}$$

Each SIF depends on only one displacement component, as opposed to the case of orthotropic material.

Consider the properties of the matrix  $[\mathbf{B}]^{-1}$ .

*Property 1.* It follows from the form of the matrix  $[\mathbf{B}]^{-1}$  that mode separation is observed at  $E_1 = E_2$  (for example, in the case of cubic symmetry), i.e.,  $K_I$  depends only on  $u_y$ ,  $K_{II}$  depends only on  $u_x$ , the same as in the case of isotropic material, but the expressions in the case of cubic symmetry are different from the isotropic material.

*Property 2.* Similarly, if  $E_1 = E_2$  (for example, for cubic symmetry), the coefficients of the matrix  $[\mathbf{B}]^{-1}$  are the same for any angle  $\varphi$ , i.e., they do not depend on it, as is the case for isotropic material.

*Property 3.* The matrix element  $(\mathbf{B}^{-1})_{33}$  is constant and does not depend on the angle  $\varphi$ .

*Property 4.* In the cases of cubic symmetry and isotropic material,  $K_I$  linearly depends on  $u_y$  with the same proportionality factor as  $K_{II}$  depends on  $u_x$ .

*Property 5.* To analyze the degree to which  $u_x$  or  $u_y$  affect  $K_I$  and  $K_{II}$  for orthotropic material, consider the passes to the limit:

$$\lim_{\frac{E_1}{E_2} \rightarrow 0} \frac{(B^{-1})_{12}}{(B^{-1})_{11}} = \lim_{\frac{E_1}{E_2} \rightarrow 0} \frac{\sqrt{\frac{E_1}{E_2}} \sin^2 \varphi + \cos^2 \varphi}{\left( 1 - \sqrt{\frac{E_1}{E_2}} \right) \sin \varphi \cos \varphi} = \text{ctg} \varphi, \quad \lim_{\frac{E_1}{E_2} \rightarrow \infty} \frac{(B^{-1})_{12}}{(B^{-1})_{11}} = \lim_{\frac{E_1}{E_2} \rightarrow 0} \frac{\left( \sqrt{\frac{E_1}{E_2}} - 1 \right) \sin^2 \varphi + 1}{\left( 1 - \sqrt{\frac{E_1}{E_2}} \right) \sin \varphi \cos \varphi} = -\text{tg} \varphi,$$

$$\lim_{\frac{E_1}{E_2} \rightarrow 0} \frac{(B^{-1})_{21}}{(B^{-1})_{22}} = \lim_{\frac{E_1}{E_2} \rightarrow 0} \frac{\sqrt{\frac{E_1}{E_2}} \cos^2 \varphi + \sin^2 \varphi}{\left(1 - \sqrt{\frac{E_1}{E_2}}\right) \sin \varphi \cos \varphi} = \operatorname{tg} \varphi, \quad \lim_{\frac{E_1}{E_2} \rightarrow \infty} \frac{(B^{-1})_{21}}{(B^{-1})_{22}} = \lim_{\frac{E_1}{E_2} \rightarrow 0} \frac{\left(\sqrt{\frac{E_1}{E_2}} - 1\right) \cos^2 \varphi + 1}{\left(1 - \sqrt{\frac{E_1}{E_2}}\right) \sin \varphi \cos \varphi} = -\operatorname{ctg} \varphi.$$

The above results confirm that this effect of  $u_x$  or  $u_y$  on  $K_I$  and  $K_{II}$  depends on the ratio of Young's moduli  $E_1/E_2$  and the rotation angle  $\varphi$ .

*Property 6.* As evident from expressions (25), the closer the root  $\sqrt{E_1/E_2}$  to unity, the smaller the elements  $(B^{-1})_{11}$ ,  $(B^{-1})_{22}$  compared to the elements  $(B^{-1})_{12}$ ,  $(B^{-1})_{21}$ . The value of  $K_I$  then largely depends on the value of  $u_y$ , and the value of  $K_{II}$  largely depends on  $u_x$ .

Analyzing the above relations, we can conclude that the degree of influence from either  $u_y$  or  $u_x$  depends on the value of the angle  $\varphi$ .

*Property 7.* Consider the determinant of the matrix  $[\mathbf{B}]^{-1}$ :

$$\det [\mathbf{B}]^{-1} = \sqrt{G_{13}G_{23}} \cdot \frac{E_1 E_2}{4B^2} \cdot \left( \left( 1 + \frac{E_1}{E_2} - 2\sqrt{\frac{E_1}{E_2}} \right) \sin^2 \varphi \cos^2 \varphi - \frac{E_1}{E_2} \sin^2 \varphi \cos^2 \varphi - \sin^2 \varphi \cos^2 \varphi - \sqrt{\frac{E_1}{E_2}} \sin^4 \varphi - \sqrt{\frac{E_1}{E_2}} \cos^4 \varphi \right) = -\sqrt{G_{13}G_{23}} \frac{E_1 \sqrt{E_1 E_2}}{4B^2}.$$

It follows from the form that the determinant of the matrix  $[\mathbf{B}]^{-1}$  takes that the SIF cannot be explicitly calculated from the displacements, if

$$B = \frac{\sqrt{2\sqrt{\frac{E_1}{E_2}} + \left(\frac{E_1}{G_{12}} - 2\nu_{12}\right)}}{2} = 0.$$

$$2\sqrt{\frac{E_1}{E_2}} + \left(\frac{E_1}{G_{12}} - 2\nu_{12}\right) = 0, \quad \frac{E_1}{G_{12}} - 2\nu_{12} < 0, \quad \frac{E_1}{G_{12}} + 2\sqrt{\frac{E_1}{E_2}} < 1.$$

This corresponds to the case when the roots in the 4th-order equation take real values, which makes all elements of the matrix  $[\mathbf{B}]^{-1}$  equal to zero; however, it was found in [15] that Eq. (16) cannot have real roots. On the other hand, if the ratio of elastic constants is such that

$$2\sqrt{\frac{E_1}{E_2}} + \left(\frac{E_1}{G_{12}} - 2\nu_{12}\right) \approx 0$$

or  $E_1$  is sufficiently small, it may be problematic to numerically calculate the matrix  $[\mathbf{B}]^{-1}$  or the SIF.

To illustrate other properties of the elements in the matrix  $[\mathbf{B}]^{-1}$ , we assume that the orthotropic material has the same properties as in Table 1, and plot the variations in the matrix elements depending on the crack's rotation angle  $\varphi$  (Fig. 2).

*Property 8.* Fig. 2 shows that all elements of the matrix  $[\mathbf{B}]^{-1}$ , except the constant  $(B^{-1})_{33}$ , vary with a period  $T = \pi$ .

The matrix elements  $(B^{-1})_{11}$ ,  $(B^{-1})_{22}$  become zero periodically, and the coefficient  $K_I$  depends only on  $u_y$ , while  $K_{II}$  depends only on  $u_x$  for the values of the angle  $\varphi = 0, \pi/2, \pi, \dots$  for the orthotropic material (as well as for the cases of cubic symmetry and isotropic material).

The graphs of matrix elements  $(B^{-1})_{12}$ ,  $(B^{-1})_{21}$  are shifted relative to each other by  $\varphi = \pi/2$ .

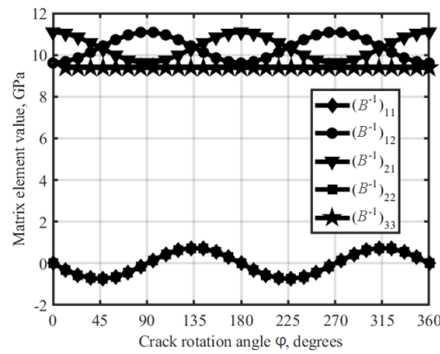


Fig. 2. Values of elements in matrix  $[B]^{-1}$  for orthotropic material as a function of the crack's rotation angle relative to its axes

*Property 9.* To analyze whether the matrix is definite, we calculate its main minors:

$$\text{minor } \Delta_1 = \frac{\sqrt{E_1 E_2}}{4B} \left( 1 - \sqrt{\frac{E_1}{E_2}} \right) \sin 2\varphi$$

can be both greater or smaller than zero;

$$\text{minor } \Delta_2 = -\frac{E_1 \sqrt{E_1 E_2}}{4B^2} < 0, \quad \Delta_3 = -\sqrt{G_{13} G_{23}} \frac{E_1 \sqrt{E_1 E_2}}{4B^2} < 0.$$

Apparently, the matrix  $[B]^{-1}$  is neither positive-definite nor negative-definite.

*Property 10.* The eigenvalues of the matrix  $[B]^{-1}$  are defined as the roots of the equation

$$\begin{vmatrix} \frac{\sqrt{E_1 E_2}}{4B} \left( 1 - \sqrt{\frac{E_1}{E_2}} \right) \sin 2\varphi - \lambda & \frac{\sqrt{E_1 E_2}}{2B} \left( \sqrt{\frac{E_1}{E_2}} \sin^2 \varphi + \cos^2 \varphi \right) & 0 \\ \frac{\sqrt{E_1 E_2}}{2B} \left( \sqrt{\frac{E_1}{E_2}} \cos^2 \varphi + \sin^2 \varphi \right) & \frac{\sqrt{E_1 E_2}}{4B} \left( 1 - \sqrt{\frac{E_1}{E_2}} \right) \sin 2\varphi - \lambda & 0 \\ 0 & 0 & \sqrt{G_{13} G_{23}} - \lambda \end{vmatrix} = 0.$$

Table 1

**Elastic properties of orthotropic material used in calculations**

Modulus, MPa		Poisson's ratio
Young's ratio	Shear modulus	
$E_1 = 20,000$	$G_{12} = 13,000$	$\nu_{12} = 0.3$
$E_2 = 25,000$	$G_{23} = 11,000$	$\nu_{23} = 0.25$
$E_3 = 10,000$	$G_{31} = 8,000$	$\nu_{31} = 0.2$

Calculating the determinant, we obtain a cubic equation with respect to  $\lambda$ :

$$(\sqrt{G_{13}G_{23}} - \lambda) \cdot (\lambda^2 - \lambda \frac{\sqrt{E_1 E_2}}{B} \left(1 - \sqrt{\frac{E_1}{E_2}}\right) \sin \varphi \cos \varphi - \frac{E_1 \sqrt{E_1 E_2}}{4B^2}) = 0. \quad (27)$$

Separating the factors and calculating the discriminant, we find the roots of the equation:

$$\begin{aligned} \lambda_1 &= \frac{\sqrt{E_1 E_2}}{2B} \left( \left(1 - \sqrt{\frac{E_1}{E_2}}\right) \sin \varphi \cos \varphi + \sqrt{\left(1 + \frac{E_1}{E_2}\right) \sin^2 \varphi \cos^2 \varphi + \frac{E_1}{E_2} (\sin^4 \varphi + \cos^4 \varphi)} \right), \\ \lambda_2 &= \frac{\sqrt{E_1 E_2}}{2B} \left( \left(1 - \sqrt{\frac{E_1}{E_2}}\right) \sin \varphi \cos \varphi - \sqrt{\left(1 + \frac{E_1}{E_2}\right) \sin^2 \varphi \cos^2 \varphi + \frac{E_1}{E_2} (\sin^4 \varphi + \cos^4 \varphi)} \right), \\ \lambda_3 &= \sqrt{G_{13}G_{23}}. \end{aligned} \quad (28)$$

Thus, one eigenvalue of the matrix  $[\mathbf{B}]^{-1}$  does not depend on the angle  $\varphi$  at all, and the other two are periodic functions of the angle  $\varphi$  with the period  $\pi$ .

#### Verification of the methods for calculating the SIF for cracks in anisotropic materials by the finite element method

The displacement method and the resulting expressions for matrix  $[\mathbf{B}]^{-1}$  were tested based on the results of the FE solution for the boundary-value problem and SIF calculations for the case of a single oblique crack in the infinite plane for a mixed fracture mode (provided that modes  $K_I$  and  $K_{II}$  exist). We considered a single crack in the infinite plane at an angle  $\varphi$  to the anisotropy axis the material, normal to the direction in which the load was applied (Fig. 3). The problem was solved in a two-dimensional statement, assuming a plane stress state.

An analytical solution for SIF is known for this problem [23]:

$$\begin{aligned} K_I &= \sigma \sqrt{\pi a} \cdot \cos^2 \varphi, \\ K_{II} &= \sigma \sqrt{\pi a} \cdot \sin \varphi \cdot \cos \varphi. \end{aligned} \quad (29)$$

The analytical solution for the infinite plane does not depend on the type of anisotropy and the values taken by the elastic moduli of the material. The problem was solved in the PANTOCRATOR FE software [32], programmed to calculate the SIF for isotropic and anisotropic materials using the methods of displacements (see Eqs. (8), (10)) and stresses (see Eqs. (13) and (15)). Quadratic 8-node finite elements were used in the calculations.

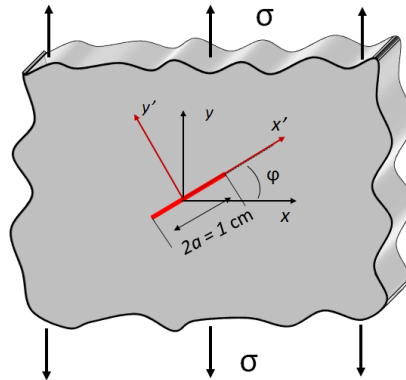


Fig. 3. Schematic for the statement of the problem on uniaxial tension of a plane with an oblique crack (highlighted in red).

The notations are the same as in Fig. 1

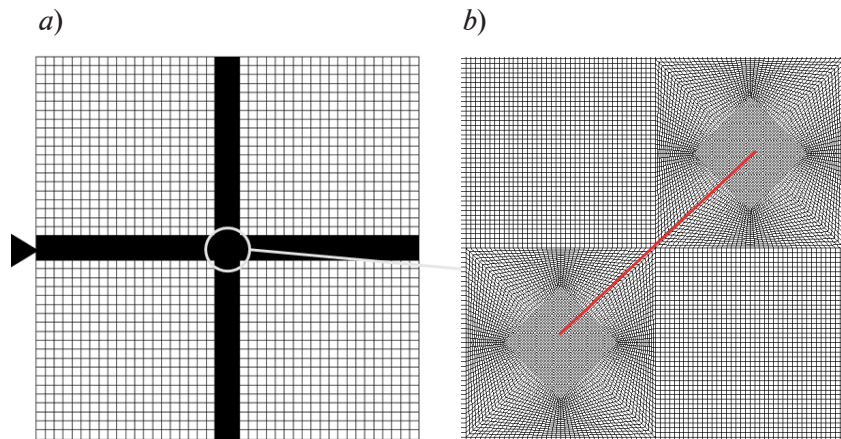


Fig. 4. Finite-element model of plate with oblique crack (a) and its central fragment (b)

FE models were constructed to compare the numerical solutions with analytical ones at different values of the angle  $\varphi$  (the crack's orientation angle relative to the material's orthotropy axes). Fig. 4 shows an example FE model with 126,000 degrees of freedom and 80 elements at the edge of the crack for the case of a square plate of finite dimensions and an inclination angle  $\varphi = 45^\circ$ .

The length and the width of the computational domain were taken to be 22 cm; the crack length was 1 cm, which is an approximation for modeling the crack's behavior in an infinite region. The plate was loaded on the upper edge with the stress  $\sigma_{yy} = 100$  MPa and clamped at the lower edge (to exclude solid-state displacements). The elastic properties of the materials used in the calculations are given in Table 2.

Fig. 5 shows a comparison of numerical results for SIFs obtained by displacement and stress extrapolation with an analytical solution for three types of material: isotropic, orthotropic and cubic.

Table 2

**Elastic properties of materials for three types of symmetry, used in FE calculations**

Material	Modulus, MPa		Poisson's ratio
	Young's ratio	Shear modulus	
Isotropic	$E = 20,000$	$G = \frac{E}{2(1+\nu)} = 7692.3$	$\nu = 0.3$
With cubic symmetry	$E = 20,000$	$G = 11,000$	$\nu = 0.3$
Orthotropic	$E_1 = 20,000$ $E_2 = 15,000$ $E_3 = 10,000$	$G_{12} = 13,000$ $G_{23} = 11,000$ $G_{31} = 8,000$	$\nu_{12} = 0.3$ $\nu_{23} = 0.25$ $\nu_{31} = 0.2$

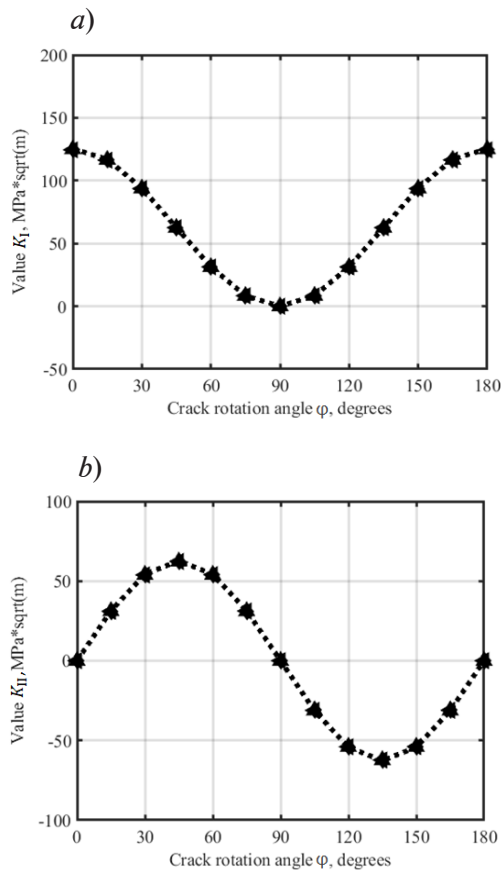


Fig. 5. Comparison of numerical solutions (symbols) for SIFs  $K_I$  (a) and  $K_{II}$  (b), obtained by the methods of displacements and stresses, with analytical solutions (dashes). The data are given for isotropic ( $\blacktriangle$ ) and orthotropic ( $\blacktriangleleft$ ) materials and for the material with cubic symmetry ( $\blacklozenge$ )

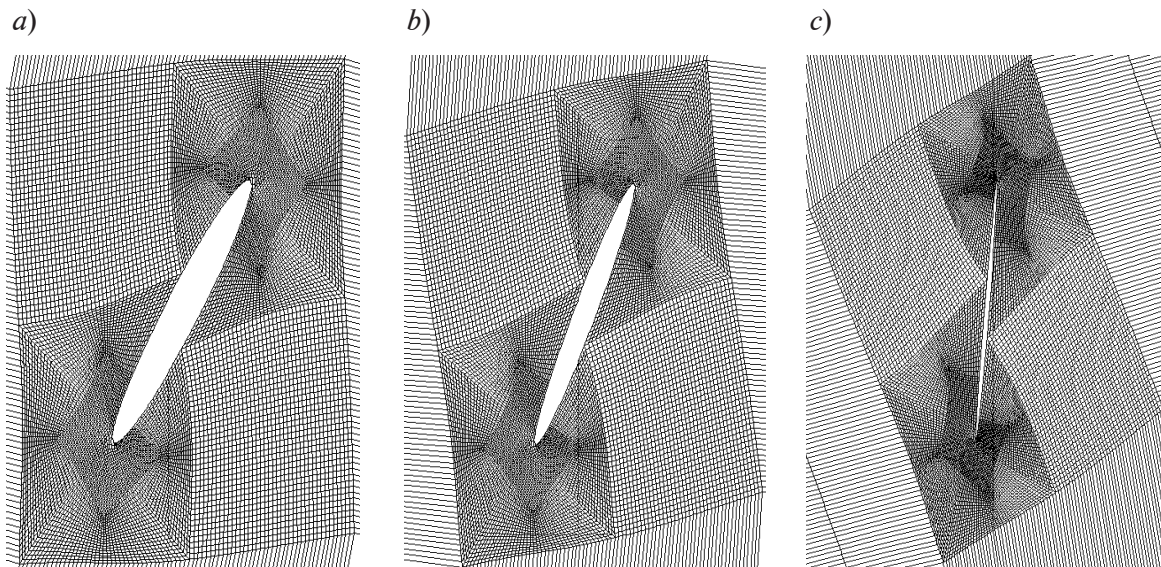


Fig. 6. Comparative results for FEM calculations of crack opening (initial inclination angle  $\varphi = 60^\circ$ ) for materials with different symmetry of elastic properties: isotropic (a), cubic (b) and orthotropic (c). The scale of displacements is magnified by 60 times



Table 3 shows the values of  $K_I$  and  $K_{II}$  corresponding to Fig. 5. Notably, the maximum error  $\delta_{max}$  for the displacement method (0.79%) exceeds that for the stress method (0.42%); the error is minimal for the isotropic material and maximal for the orthotropic one. However, the error does not exceed 0.8% for all cases considered, confirming that both methods have a high accuracy.

Fig. 6 shows the differences in crack opening for different cases of material anisotropy with the crack inclination angle  $\varphi = 60^\circ$ .

FEM calculations performed for three cases of elastic symmetry in the material indicate that the crack opens to the maximum in the isotropic case, to the minimum in the orthotropic case, other conditions given by specific values of the elastic parameters being equal.

Table 3

**Comparison of analytical and numerical solutions for three types of material**

$\varphi, ^\circ$	Analytical solution		Numerical solution by method of					
			displacements			stresses		
	$K_I$	$K_{II}$	$K_I$	$K_{II}$	$\delta_{max}$	$K_I$	$K_{II}$	$\delta_{max}$
MPa·m <sup>1/2</sup>				%	MPa·m <sup>1/2</sup>		%	
<i>For isotropic material</i>								
0	125.33	0	124.96	0.0005	<b>0.29</b>	125.05	0.0003	<b>0.22</b>
30	93.99	54.27	93.70	53.93	<b>0.62</b>	93.93	54.26	<b>0.07</b>
60	31.33	54.27	31.22	53.92	<b>0.64</b>	31.30	54.25	<b>0.10</b>
90	0	0	< 0.0001	0.0002	<b>0.02</b>	< 0.0001	< 0.0001	< <b>0.01</b>
120	31.33	-54.27	31.22	-53.91	<b>0.65</b>	31.28	-54.23	<b>0.15</b>
150	93.99	-54.27	93.70	-53.93	<b>0.62</b>	93.93	-54.26	<b>0.07</b>
180	125.33	0	124.96	0.0005	<b>0.29</b>	125.05	0.0003	<b>0.22</b>
<i>For material with cubic symmetry</i>								
0	125.33	0	124.77	0.004	<b>0.22</b>	125.07	0.003	<b>0.20</b>
30	93.99	54.27	93.68	53.89	0.20	93.90	54.22	<b>0.10</b>
60	31.33	54.27	31.26	53.94	0.60	31.34	54.29	<b>0.04</b>
90	0	0	< 0.0001	0.0002	0.02	< 0.0001	< 0.0001	< <b>0.01</b>
120	31.33	-54.27	31.25	-53.94	0.60	31.31	-54.29	<b>0.07</b>
150	93.99	-54.27	93.68	-53.89	0.70	93.90	-54.22	<b>0.10</b>
180	125.33	0	124.77	0.004	0.45	125.07	0.003	<b>0.45</b>
<i>For orthotropic material</i>								
0	125.33	0	124.50	0.006	0.66	124.80	0.007	<b>0.42</b>
30	93.99	54.27	93.61	53.84	0.79	93.83	54.23	<b>0.18</b>
60	31.33	54.27	31.31	53.95	0.58	31.40	54.30	<b>0.20</b>
90	0	0	< 0.0001	0.0002	0.02	< 0.0001	< 0.0001	< <b>0.01</b>
120	31.33	-54.27	31.29	-53.95	0.58	31.35	-54.30	<b>0.08</b>
150	93.99	-54.27	93.61	-53.84	0.79	93.83	-54.23	<b>0.18</b>
180	125.33	0	124.50	0.006	0.66	124.80	0.0068	<b>0.42</b>

Notations:  $\varphi$  is the crack inclination angle to the axis  $x$ ;  $\delta_{max}$  is the maximum relative error of either of the two factors  $K_I$  and  $K_{II}$  (stress intensity factors for fracture modes I and II), taken relative to the result of the analytical solution.



## Conclusions

Considering the case of a plane stress state, we have obtained explicit expressions for the roots of the equation of the 4th degree, defining the elements of the influence matrix accounting for three components of the relative displacement vector of the crack edges versus three stress intensity factors  $[\mathbf{B}]^{-1}$  in terms of the elastic constants of materials with orthotropic or cubic symmetry. We have carried out a systematic study of the properties of the influence matrix  $[\mathbf{B}]^{-1}$ . The absence of mode mixing has been established for a material with cubic symmetry.

In addition, the SIF values were calculated for an oblique single crack in a plane stress state using two numerical methods: extrapolation of displacements and stresses to the tip of the crack for different orientations of the crack in the plane relative to the anisotropy axes of the material. The results of numerical solutions agree well with the analytical solution for the isotropic, cubic and orthotropic materials (the error did not exceed 0.8% in all cases). We have established that the method for calculating the SIF in terms of stress extrapolation to the tip of the crack has a higher accuracy than the method based on displacement extrapolation.

Finite element modeling of a plate with an oblique crack suggests that if the highest values of Young's modulus are equal, the crack edges open to the maximum extent in the isotropic material, and to the minimum in the orthotropic material.

The methods of displacement and stress extrapolation can be recommended for estimating the SIF in crack growth simulations and calculations of crack resistance in single-crystal blades of gas turbines.

## REFERENCES

1. **Shalin R. E., Svetlov I. L., Kachalov E. B., et al.**, Monokristally nikelovykh zharoprochnykh splavov [Single crystals of nickel heat-resistant alloys], Mashinostroyeniye, Moscow, 1997 (in Russian).
2. **Wilson B. C., Hickman J. A., Fuchs G. E.**, The effect of solution heat treatment on a single-crystal Ni-based superalloy, JOM. 55 (3) (2003) 35–40.
3. **Hodinev I. A., Monin S. A.**, Anisotropy of low cycle fatigue characteristics of single-crystal heat-resistant nickel alloys, Proceedings of VIAM. (10 (92)) (2020) 97–105 (in Russian).
4. **Getsov L. B.**, Materialy i prochnost detaley gazovykh turbin [Materials and strength of gas turbine parts], in 2 Vols., Vol. 1, Gas Turbine Technologies Publishing, Rybinsk, 2010 (in Russian).
5. **Getsov L. B., Semenov A. S., Ignatovich I. A.**, Thermal fatigue analysis of turbine discs on the base of deformation criterion, Int. J. Fatig. 97 (April) (2017) 88–97.
6. **Wang R., Zhang B., Hu D., et al.**, A critical-plane-based thermomechanical fatigue lifetime prediction model and its application in nickel-based single-crystal turbine blades, Mater. High Temperat. 36 (4) (2019) 325–334.
7. **Glotka A. A., Gayduk S. V.**, Prediction of the properties of single-crystal heat-resistance nickel alloys, Science & Progress of Transport. Bulletin of Dnepropetrovsk National University of Railway Transport. (2(80)) (2019) 91–100 (in Russian).
8. **Bondarenko Yu. A., Kolodyazhny M. Yu., Echin A. B., Narskiy A. R.**, Directional solidification, structure and properties of natural composite based on eutectic Nb-Si at working temperatures up to 1350 °C for the blades of gas turbine engines, Proceedings of VIAM. (1 (61)) (2018) 3–14 (in Russian).
9. **Bondarenko Yu. A.**, Trends in the development of high-temperature metal materials and technologies in the production of modern aircraft gas turbine engines, Aviation Materials and Technologies. (2 (55)) (2019) 3–11 (in Russian).
10. **Semenov A. S., Grishchenko A. I., Kolotnikov M. E., Getsov L. B.**, Finite-element analysis of thermal fatigue of gas turbine blades, Part 1. Material models, fracture criteria, identification, Vestnik UGATU [USATU Bulletin]. 23 (1 (83)) (2019) 70–81 (in Russian).
11. **Semenov A. S., Grishchenko A. I., Kolotnikov M. E., Getsov L. B.**, Finite-element analysis of thermal fatigue of gas turbine blades, Part 2. Results of computations, Vestnik UGATU [USATU Bulletin]. 23 (2 (84)) (2019) 61–74 (in Russian).
12. **Getsov L. B., Semenov A. S., Besschetnov V. A., et al.**, Long-term strength determination for cooled blades made of monocrystalline superalloys, Therm. Eng. 64 (4) (2017) 280–287.
13. **Getsov L. B., Mikhaylov V. E., Semenov A. S., et al.**, Raschetnoye opredeleniye resursa rabochikh i napravlyayushchikh lopatok GTU. Chast 1. Polikristallicheskiye materialy [Design determination of the work life of operating and guide blades of gas-turbine installations. Part 1. Polycrystalline materials], Gas Turbine Technologies. (7) (2011) 24–30 (in Russian).

14. **Getsov L. B., Mikhaylov V. E., Semenov A. S., et al.**, Raschetnoye opredeleniye resursa rabochikh i napravlyayushchikh lopatok GTU. Chast 2. Monokristallicheskiye materialy [Computational determination of the work life of operating and guide blades of gas-turbine units. Part 1. Monocrystalline materials], Gas Turbine Technologies. (8) (2011) 18–25 (in Russian).
15. **Kuzmina N. A., Pyankova L. A.**, Control of crystallographic orientation of monocrystalline nickel castings heat-resistant alloys by X-ray diffractometry, Proceedings of VIAM. (12 (84)) (2019) 11–19 (in Russian).
16. **Semenov A. S., Semenov S. G., Nazarenko A. A., Getsov L. B.**, Computer simulation of fatigue, creep and thermal fatigue cracks propagation in gas turbine blades, Mater. Technol. 46 (3) (2012) 197–203.
17. **Semenov A. S., Semenov S. G., Getsov L. B.**, Methods of computational determination of growth rates of fatigue, creep, and thermal fatigue cracks in poli- and monocrystalline blades of gas-turbine units, Strength Mater. 47 (2) (2015) 268–290.
18. **Savikovskii A. V., Semenov A. S., Getsov L. B.**, Coupled thermo-electro-mechanical modeling of thermal fatigue of single-crystal corset samples, Mater. Phys. Mech. 2019. Vol. 42 (3) (2019) 296–310.
19. **Savikovskii A. V., Semenov A. S., Getsov L. B.**, Crystallographic orientation, delay time and mechanical constants influence on thermal fatigue strength of single-crystal nickel superalloys, Mater. Phys. Mech. 44 (1) (2020) 125–136.
20. **Lekhnitsky S. G.**, Teoriya uprugosti anizotropnogo tela [Theory of elasticity of an anisotropic elastic body], Nauka, Moscow, 1977 (in Russian).
21. **Martynov N. I.**, Complex form of Hooke's law of anisotropic elastic body, Mechanics of Solids. 55 (4) (2020) 514–535.
22. **Kachanov M. L.**, Osnovy mekhaniki razrusheniya [Fundamentals of fracture mechanics]. Nauka, Moscow, 1974, Pp. 223–226 (in Russian).
23. **Sih G. C., Paris P. C., Irwin G. R.**, On cracks in rectilinearly anisotropic bodies, Int. J. Fract. 1 (3) (1965) 189–203.
24. **Judt P. O., Ricoeur A., Linek G.**, Crack path prediction in rolled aluminum plates with fracture toughness orthotropy and experimental validation, Eng. Fract. Mech. 138 (April) (2015) 33–48.
25. **Banks-Sills L., Hershkovitz I., Wawrzynek P. A., et al.**, Methods for calculating stress intensity factors in anisotropic materials: Part I:  $z = 0$  is a symmetric plane, Eng. Fract. Mech. 72 (15) (2005) 2328–2358.
26. **Semenov S. G., Semenov A. S., Getsov L. B., et al.**, Application of linear and nonlinear fracture mechanics criteria for crack propagation analysis in single crystal bodies, Proc. XLI Int. Summer School–Conf. “Advanced Problems in Mechanics (APM-2013)” St. Petersburg, Russia, July 2–6 (2013) 75–82.
27. **Ranjan S., Arakere N. K.**, a fracture-mechanics-based methodology for fatigue life prediction of single crystal nickel-based superalloys, J. Eng. Gas Turbines Power. 2008 130 (3) (2008) 032501.
28. **Khansari N. M., Fakoor M., Berto F.**, Probabilistic micromechanical damage model for mixed-mode I/II fracture investigation of composite materials, Theor. Appl. Fract. Mech. 99 (February) (2019) 177–193.
29. **Cao J., Li F., Ma H., Sun Z.**, Study of anisotropic crack growth behavior for aluminum alloy 7050-T7451, Eng. Fract. Mech. 2018, Vol. 196 (1 June) (2018) 98–112.
30. **Fakoor M., Shavsavar S.**, The effect of T-stress on mixed mode I/II fracture of composite materials: Reinforcement isotropic solid model in combination with maximum shear stress theory, Int. J. Solids & Struct. 229 (15 October) (2021) 111145.
31. **Fakoor M., Farid H. M.**, Mixed-mode I/II fracture criterion for crack initiation assessment of composite materials, Acta Mechanica. 230 (1) (2019) 281–301.
32. **Semenov A. S.**, PANTOCRATOR – konechno-elementnyy programmnyy kompleks, oriyentirovanny na resheniye nelineynykh zadach mekhaniki [PANTOCRATOR – finite-element program specialized on the solution of non-linear problems of solid body mechanics], In: Proc. The V-th Int. Conf. “Scientific and engineering problems of reliability and service life of structures and methods of their decision”, St. Petersburg Polytechnical University Publishing, St. Petersburg (2003) 466–480.



## СПИСОК ЛИТЕРАТУРЫ

1. Шалин Р. Е., Светлов И. Л., Качалов Е. Б., Толораия В. Н., Гаврилин В. С. Монокристаллы никелевых жаропрочных сплавов. М.: Машиностроение. 336 .1997 с.
2. Wilson B. C., Hickman J. A., Fuchs G. E. The effect of solution heat treatment on a single-crystal Ni-based superalloy // The Journal of the Minerals, Metals & Materials Society. 2003. Vol. 55. No. 3. Pp. 35–40.
3. Ходинев И. А., Мониин С. А. Анизотропия характеристик малоциклового усталости монокристаллических жаропрочных никелевых сплавов // Труды ВИАМ (Всероссийский НИИ авиационных материалов). 92) 10 № .2020). С. 105–97.
4. Гецов Л. Б. Материалы и прочность деталей газовых турбин. В 2 тт. Т. 1. Рыбинск: Издат. дом «Газотурбинные технологии», 2010. 605 с.
5. Getsov L. B., Semenov A. S., Ignatovich I. A. Thermal fatigue analysis of turbine discs on the base of deformation criterion // International Journal of Fatigue. 2017. Vol. 97. April. Pp. 88–97.
6. Wang R., Zhang B., Hu D., Jiang K., Mao J., Jing F. A critical-plane-based thermomechanical fatigue lifetime prediction model and its application in nickel-based single-crystal turbine blades // Materials at High Temperatures. 2019. Vol. 36. No. 4. pp. 325–334.
7. Глотка А. А., Гайдук С. В. Прогнозирование свойств монокристаллических жаропрочных никелевых сплавов // Наука и прогресс транспорта. Вестник Днепропетровского национального университета железнодорожного транспорта. 80) 2 № .2019). С. 91–100.
8. Бондаренко Ю. А., Колодяжный М. Ю., Ечин А. Б., Нарский А. Р. Направленная кристаллизация, структура и свойства естественного композита на основе эвтектики Nb-Si на рабочие температуры до 1350 °С для лопаток ГТД // Труды ВИАМ. 2018. № 1 (61). С. 3–14.
9. Бондаренко Ю. А. Тенденция развития высокотемпературных металлических материалов и технологий при создании современных авиационных газотурбинных двигателей // Авиационные материалы и технологии. 55) 2 № .2019). С. 11–3.
10. Семенов А. С., Грищенко А. И., Колотников М. Е., Гецов Л. Б. Конечный элементный анализ термоциклической прочности лопаток газовых турбин Ч. 1. Модели материала, критерии разрушения, идентификация параметров // Вестник УГАТУ (Уфимский государственный авиационный технический университет). 2019. Т. 83) 1 № .23). С. 70–81.
11. Семенов А. С., Грищенко А. И., Колотников М. Е., Гецов Л. Б. Конечный элементный анализ термоциклической прочности лопаток газовых турбин. Ч. 2. Результаты расчетов // Вестник УГАТУ. 2019. Т. 23. № 2 (84). С. 61–74.
12. Гецов Л. Б., Семенов А. С., Бессчетнов В. А., Грищенко А. И., Семанов С. Г. Методика определения длительной прочности охлаждаемых лопаток из монокристаллических жаропрочных сплавов // Теплоэнергетика. 4 № .2017. С. 56–48.
13. Гецов Л. Б., Михайлов В. Е., Семенов А. С., Кривоносова В. В., Ножницкий Ю. А., Блишник Б. С., Магеррамова Л. А. Расчетное определение ресурса рабочих и направляющих лопаток ГТУ. Ч. 1. Поликристаллические материалы // Газотурбинные технологии. 2011. № 7. С. 24–30.
14. Гецов Л. Б., Михайлов В. Е., Семенов А. С., Кривоносова В. В., Ножницкий Ю. А., Блишник Б. С., Магеррамова Л. А. Расчетное определение ресурса рабочих и направляющих лопаток ГТУ. Ч. 2. Монокристаллические материалы // Газотурбинные технологии. 2011. № 8. С. 18–25.
15. Кузьмина Н. А., Пьянкова Л. А. Контроль кристаллографической ориентации монокристаллических отливок никелевых жаропрочных сплавов методом рентгеновской дифрактометрии // Труды ВИАМ. 2019. № 12 (84). С. 11–19.
16. Semenov A., Semenov S., Nazarenko A., Getsov L. Computer simulation of fatigue, creep and thermal-fatigue cracks propagation in gas-turbine blades // Materials and Technology. 2012. Vol. 46. No. 3. Pp. 197–203.
17. Семенов А. С., Семенов С. Г., Гецов Л. Б. Методы расчетного определения скорости роста трещин усталости, ползучести и термоусталости в поли- и монокристаллических лопатках ГТУ // Проблемы прочности. 2015. № 2. С. 61–87.
18. Savikovskii A. V., Semenov A. S., Getsov L. B. Coupled thermo-electro-mechanical modeling of thermal fatigue of single-crystal corset samples // Materials Physics and Mechanics. 2019. Vol. 42. No. 3. Pp. 296–310.

19. **Savikovskii A. V., Semenov A. S., Getsov L. B.** Crystallographic orientation, delay time and mechanical constants influence on thermal fatigue strength of single-crystal nickel superalloys // *Materials Physics and Mechanics*. 2020. Vol. 44. No. 1. Pp. 125–136.
20. **Лехницкий С. Г.** Теория упругости анизотропного тела. М.: Наука, 1977. 416 с.
21. **Мартынов Н. И.** Комплексная форма закона Гука анизотропного упругого тела // *Известия РАН. Механика твердого тела*. 4 № .2020. С. 71–95.
22. **Качанов Л. М.** Основы механики разрушения. М.: Наука, 1974. С. 223–226.
23. **Sih G. C., Paris P. C., Irwin G. R.** On cracks in rectilinearly anisotropic bodies // *International Journal of Fracture Mechanics*. 1965. Vol. 1. No. 3. Pp. 189–203.
24. **Judt P. O., Ricoeur A., Linek G.** Crack path prediction in rolled aluminum plates with fracture toughness orthotropy and experimental validation // *Engineering Fracture Mechanics*. 2015. Vol. 138. April. Pp. 33–48.
25. **Banks-Sills L., Hershkovitz I., Wawrzynek P. A., Eliasi R., Ingraffea A. R.** Methods for calculating stress intensity factors in anisotropic materials: Part I:  $z = 0$  is a symmetric plane // *Engineering Fracture Mechanics*. 2005. Vol. 72. No. 15. Pp. 2328–2358.
26. **Semenov S. G., Semenov A. S., Getsov L. B., Melnikov B. E.** Application of linear and nonlinear fracture mechanics criteria for crack propagation analysis in single crystal bodies // *Proceedings of XLI International Summer School –Conference “Advanced Problems in Mechanics (APM-2013)” Russia, St. Petersburg, July 2–6, 2013*. Pp. 75–82.
27. **Ranjan S., Arakere N. K.** A fracture-mechanics-based methodology for fatigue life prediction of single crystal nickel-based superalloys // *Journal of Engineering for Gas Turbines and Power*. 2008. Vol. 130. No. 3. P. 032501.
28. **Khansari N. M., Fakoor M., Berto F.** Probabilistic micromechanical damage model for mixed-mode I/II fracture investigation of composite materials // *Theoretical and Applied Fracture Mechanics*. 2019, Vol. 99. February. Pp. 177–193.
29. **Cao J., Li F., Ma H., Sun Z.** Study of anisotropic crack growth behavior for aluminum alloy 7050-T7451 // *Engineering Fracture Mechanics*. 2018. Vol. 196. 1 June. Pp. 98–112.
30. **Fakoor M., Shavsavar S.** The effect of T-stress on mixed mode I/II fracture of composite materials: Reinforcement isotropic solid model in combination with maximum shear stress theory // *International Journal of Solids and Structures*. 2021. Vol. 229. 15 October. P. 111145.
31. **Fakoor M., Farid H. M.** Mixed-mode I/II fracture criterion for crack initiation assessment of composite materials // *Acta Mechanica*. 2019. Vol. 230. No. 1. Pp. 281–301.
32. **Семенов А. С.** PANTOCRATOR – конечно-элементный программный комплекс, ориентированный на решение нелинейных задач механики // *Труды V-ой Международной конференции «Научно-технические проблемы прогнозирования надежности и долговечности конструкций»*. СПб.: Изд-во СПбГПУ, 2003. С. 466 –480.

## THE AUTHORS

### **SAVIKOVSKII Artem V.**

*Peter the Great St. Petersburg Polytechnic University*  
29 Politechnicheskaya St., St. Petersburg, 195251, Russia  
savikovskij.av@edu.spbstu.ru  
ORCID: 0000-0003-1710-1943

### **SEMENOV Artem S.**

*Peter the Great St. Petersburg Polytechnic University*  
29 Politechnicheskaya St., St. Petersburg, 195251, Russia  
Semenov.Artem@gmail.com  
ORCID: 0000-0002-8225-3487

**СВЕДЕНИЯ ОБ АВТОРАХ**

**САВИКОВСКИЙ Артем Викторович** – аспирант кафедры «Механика и процессы управления» Санкт-Петербургского политехнического университета Петра Великого.

195251, Россия, г. Санкт-Петербург, Политехническая ул., 29

savikovskij.av@edu.spbstu.ru

ORCID: 0000-0003-1710-1943

**СЕМЕНОВ Артем Семенович** – кандидат физико-математических наук, заведующий кафедрой сопротивления материалов Санкт-Петербургского политехнического университета Петра Великого.

195251, Россия, г. Санкт-Петербург, Политехническая ул., 29

Semenov.Artem@googlemail.com

ORCID: 0000-0002-8225-3487

*Received 20.01.2022. Approved after reviewing 22.04.2022. Accepted 22.04.2022.*

*Статья поступила в редакцию 20.01.2022. Одобрена после рецензирования 22.04.2022. Принята 22.04.2022.*